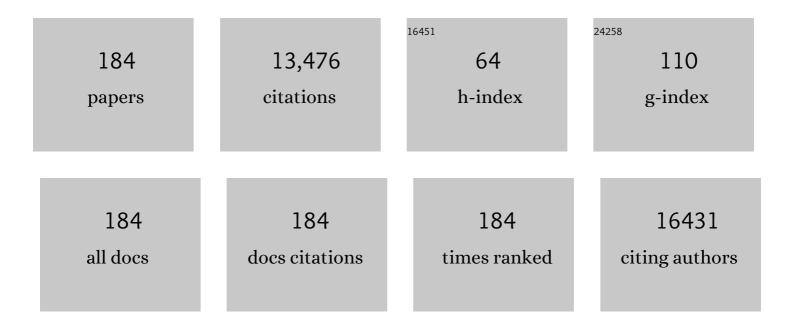
## Hongen Wang

List of Publications by Year in descending order

Source: https://exaly.com/author-pdf/5678612/publications.pdf Version: 2024-02-01



#	Article	IF	CITATIONS
1	Applications of hierarchically structured porous materials from energy storage and conversion, catalysis, photocatalysis, adsorption, separation, and sensing to biomedicine. Chemical Society Reviews, 2016, 45, 3479-3563.	38.1	1,134
2	Hierarchically porous materials: synthesis strategies and structure design. Chemical Society Reviews, 2017, 46, 481-558.	38.1	1,030
3	Hierarchically Structured Porous Materials for Energy Conversion and Storage. Advanced Functional Materials, 2012, 22, 4634-4667.	14.9	796
4	MoSe2 nanosheets perpendicularly grown on graphene with Mo–C bonding for sodium-ion capacitors. Nano Energy, 2018, 47, 224-234.	16.0	358
5	Emerging of Heterostructure Materials in Energy Storage: A Review. Advanced Materials, 2021, 33, e2100855.	21.0	308
6	Tunable Band Gaps and p-Type Transport Properties of Boron-Doped Graphenes by Controllable Ion Doping Using Reactive Microwave Plasma. ACS Nano, 2012, 6, 1970-1978.	14.6	244
7	Probing effective photocorrosion inhibition and highly improved photocatalytic hydrogen production on monodisperse PANI@CdS core-shell nanospheres. Applied Catalysis B: Environmental, 2016, 188, 351-359.	20.2	219
8	Growth, patterning and alignment of organolead iodide perovskite nanowires for optoelectronic devices. Nanoscale, 2015, 7, 4163-4170.	5.6	181
9	Bio-inspired Murray materials for mass transfer and activity. Nature Communications, 2017, 8, 14921.	12.8	176
10	One-Dimensional Metal Oxide Nanotubes, Nanowires, Nanoribbons, and Nanorods: Synthesis, Characterizations, Properties and Applications. Critical Reviews in Solid State and Materials Sciences, 2012, 37, 1-74.	12.3	170
11	Walnut-like Porous Core/Shell TiO <sub>2</sub> with Hybridized Phases Enabling Fast and Stable Lithium Storage. ACS Applied Materials & Interfaces, 2017, 9, 10652-10663.	8.0	169
12	Single-crystal α-MnO2nanorods: synthesis and electrochemical properties. Nanotechnology, 2007, 18, 115616.	2.6	166
13	Hierarchically structured porous materials: synthesis strategies and applications in energy storage. National Science Review, 2020, 7, 1667-1701.	9.5	164
14	Tailoring CuO nanostructures for enhanced photocatalytic property. Journal of Colloid and Interface Science, 2012, 384, 1-9.	9.4	162
15	Lamellar MoSe <sub>2</sub> nanosheets embedded with MoO <sub>2</sub> nanoparticles: novel hybrid nanostructures promoted excellent performances for lithium ion batteries. Nanoscale, 2016, 8, 17902-17910.	5.6	143
16	rGO/SnS <sub>2</sub> /TiO <sub>2</sub> heterostructured composite with dual-confinement for enhanced lithium-ion storage. Journal of Materials Chemistry A, 2017, 5, 25056-25063.	10.3	136
17	Well Shaped Mn <sub>3</sub> O <sub>4</sub> Nanoâ€octahedra with Anomalous Magnetic Behavior and Enhanced Photodecomposition Properties. Small, 2011, 7, 475-483.	10.0	131
18	Design of coherent anode materials with 0D Ni <sub>3</sub> S <sub>2</sub> nanoparticles self-assembled on 3D interconnected carbon networks for fast and reversible sodium storage. Journal of Materials Chemistry A, 2017, 5, 7394-7402.	10.3	125

#	Article	IF	CITATIONS
19	Design of new anode materials based on hierarchical, three dimensional ordered macro-mesoporous TiO2 for high performance lithium ion batteries. Journal of Materials Chemistry A, 2014, 2, 9699.	10.3	124
20	Facile synthesis of porous LiMn2O4 spheres as positive electrode for high-power lithium ion batteries. Journal of Power Sources, 2012, 198, 251-257.	7.8	122
21	Phosphorized SnO <sub>2</sub> /graphene heterostructures for highly reversible lithium-ion storage with enhanced pseudocapacitance. Journal of Materials Chemistry A, 2018, 6, 3479-3487.	10.3	117
22	Reversible and fast Na-ion storage in MoO2/MoSe2 heterostructures for high energy-high power Na-ion capacitors. Energy Storage Materials, 2018, 12, 241-251.	18.0	117
23	SnS <sub>2</sub> /TiO <sub>2</sub> nanohybrids chemically bonded on nitrogen-doped graphene for lithium–sulfur batteries: synergy of vacancy defects and heterostructures. Nanoscale, 2018, 10, 15505-15512.	5.6	116
24	3D interconnected macro-mesoporous electrode with self-assembled NiO nanodots for high-performance supercapacitor-like Li-ion battery. Nano Energy, 2016, 22, 269-277.	16.0	115
25	3D Ferroconcreteâ€Like Aminated Carbon Nanotubes Network Anchoring Sulfur for Advanced Lithium–Sulfur Battery. Advanced Energy Materials, 2018, 8, 1801066.	19.5	115
26	Encapsulating NiS nanocrystal into nitrogen-doped carbon framework for high performance sodium/potassium-ion storage. Chemical Engineering Journal, 2020, 392, 123675.	12.7	115
27	Ultralong Cu(OH)2 and CuO nanowire bundles: PEG200-directed crystal growth for enhanced photocatalytic performance. Journal of Colloid and Interface Science, 2010, 348, 303-312.	9.4	113
28	Hydrothermal synthesis of hierarchical SnO <sub>2</sub> microspheres for gas sensing and lithium-ion batteries applications: Fluoride-mediated formation of solid and hollow structures. Journal of Materials Chemistry, 2012, 22, 2140-2148.	6.7	112
29	Manganese dioxide nanosheet functionalized sulfur@PEDOT core–shell nanospheres for advanced lithium–sulfur batteries. Journal of Materials Chemistry A, 2016, 4, 9403-9412.	10.3	112
30	Sulfur-deficient MoS <sub>2</sub> grown inside hollow mesoporous carbon as a functional polysulfide mediator. Journal of Materials Chemistry A, 2019, 7, 12068-12074.	10.3	112
31	Rapid Microwave Synthesis of Porous TiO <sub>2</sub> Spheres and Their Applications in Dye-Sensitized Solar Cells. Journal of Physical Chemistry C, 2011, 115, 10419-10425.	3.1	111
32	Oxygen-deficient titanium dioxide as a functional host for lithium–sulfur batteries. Journal of Materials Chemistry A, 2019, 7, 10346-10353.	10.3	109
33	Engineering single crystalline Mn3O4 nano-octahedra with exposed highly active {011} facets for high performance lithium ion batteries. Nanoscale, 2014, 6, 6819.	5.6	99
34	Hydrothermal synthesis of ordered single-crystalline rutile TiO2 nanorod arrays on different substrates. Applied Physics Letters, 2010, 96, .	3.3	97
35	Amorphous/crystalline hybrid MoO <sub>2</sub> nanosheets for high-energy lithium-ion capacitors. Chemical Communications, 2017, 53, 10723-10726.	4.1	97
36	Hierarchical mesoporous urchin-like Mn3O4/carbon microspheres with highly enhanced lithium battery performance by in-situ carbonization of new lamellar manganese alkoxide (Mn-DEG). Nano Energy, 2015, 12, 833-844.	16.0	96

#	Article	IF	CITATIONS
37	2D ZnO mesoporous single-crystal nanosheets with exposed {0001} polar facets for the depollution of cationic dye molecules by highly selective adsorption and photocatalytic decomposition. Applied Catalysis B: Environmental, 2016, 181, 138-145.	20.2	95
38	Pt supported on Mo2C particles with synergistic effect and strong interaction force for methanol electro-oxidation. Electrochimica Acta, 2013, 95, 218-224.	5.2	92
39	Anchoring ultrafine metallic and oxidized Pt nanoclusters on yolk-shell TiO2 for unprecedentedly high photocatalytic hydrogen production. Nano Energy, 2017, 38, 118-126.	16.0	91
40	Mussel-inspired coating of energetic crystals: A compact core–shell structure with highly enhanced thermal stability. Chemical Engineering Journal, 2017, 309, 140-150.	12.7	91
41	High photocatalytic activity enhancement of titania inverse opal films by slow photon effect induced strong light absorption. Journal of Materials Chemistry A, 2013, 1, 15491.	10.3	90
42	PtO nanodots promoting Ti3C2 MXene in-situ converted Ti3C2/TiO2 composites for photocatalytic hydrogen production. Chemical Engineering Journal, 2021, 420, 129695.	12.7	88
43	Structural engineering of tin sulfides anchored on nitrogen/phosphorus dual-doped carbon nanofibres in sodium/potassium-ion batteries. Carbon, 2022, 189, 46-56.	10.3	86
44	Hybrid photovoltaic cells based on ZnO/Sb <sub>2</sub> S <sub>3</sub> /P3HT heterojunctions. Physica Status Solidi (B): Basic Research, 2012, 249, 627-633.	1.5	85
45	High Efficiency CdS/CdSe Quantum Dot Sensitized Solar Cells with Two ZnSe Layers. ACS Applied Materials & Interfaces, 2016, 8, 34482-34489.	8.0	85
46	Superior Pseudocapacitive Lithium-Ion Storage in Porous Vanadium Oxides@C Heterostructure Composite. ACS Applied Materials & Interfaces, 2017, 9, 43665-43673.	8.0	83
47	MOF-derived nitrogen-doped core–shell hierarchical porous carbon confining selenium for advanced lithium–selenium batteries. Nanoscale, 2019, 11, 6970-6981.	5.6	83
48	Threeâ€Ðimensionally Ordered Macroporous Titania with Structural and Photonic Effects for Enhanced Photocatalytic Efficiency. ChemSusChem, 2011, 4, 1481-1488.	6.8	81
49	An oxygen-deficient vanadium oxide@N-doped carbon heterostructure for sodium-ion batteries: insights into the charge storage mechanism and enhanced reaction kinetics. Journal of Materials Chemistry A, 2020, 8, 3450-3458.	10.3	81
50	Hollow Co–Mo–Se nanosheet arrays derived from metal-organic framework for high-performance supercapacitors. Journal of Power Sources, 2021, 490, 229532.	7.8	79
51	In-Situ Growing Mesoporous CuO/O-Doped g-C <sub>3</sub> N <sub>4</sub> Nanospheres for Highly Enhanced Lithium Storage. ACS Applied Materials & Interfaces, 2019, 11, 32957-32968.	8.0	78
52	Oneâ€Pot Synthesis of Catalytically Stable and Active Nanoreactors: Encapsulation of Size ontrolled Nanoparticles within a Hierarchically Macroporous Core@Ordered Mesoporous Shell System. Advanced Materials, 2009, 21, 1368-1372.	21.0	77
53	Large-scale fabrication of graphene-wrapped FeF3 nanocrystals as cathode materials for lithium ion batteries. Nanoscale, 2013, 5, 6338.	5.6	77
54	Facile synthesis and electrochemical characterization of porous and dense TiO2 nanospheres for lithium-ion battery applications. Journal of Power Sources, 2011, 196, 6394-6399.	7.8	75

#	Article	IF	CITATIONS
55	Highly porous TiO2 hollow microspheres constructed by radially oriented nanorods chains for high capacity, high rate and long cycle capability lithium battery. Nano Energy, 2015, 16, 339-349.	16.0	73
56	Synergistic coupling of lamellar MoSe2 and SnO2 nanoparticles via chemical bonding at interface for stable and high-power sodium-ion capacitors. Chemical Engineering Journal, 2018, 354, 1164-1173.	12.7	73
57	Tracing the slow photon effect in a ZnO inverse opal film for photocatalytic activity enhancement. Journal of Materials Chemistry A, 2014, 2, 5051.	10.3	70
58	Impacts of surface or interface chemistry of ZnSe passivation layer on the performance of CdS/CdSe quantum dot sensitized solar cells. Nano Energy, 2017, 32, 433-440.	16.0	70
59	Carbon-bonded, oxygen-deficient TiO2 nanotubes with hybridized phases for superior Na-ion storage. Chemical Engineering Journal, 2018, 350, 201-208.	12.7	70
60	Tubular MoO2 organized by 2D assemblies for fast and durable alkali-ion storage. Energy Storage Materials, 2018, 11, 161-169.	18.0	69
61	Hierarchy Design in Metal Oxides as Anodes for Advanced Lithiumâ€lon Batteries. Small Methods, 2018, 2, 1800171.	8.6	69
62	Towards high-performance all-solid-state asymmetric supercapacitors: A hierarchical doughnut-like Ni3S2@PPy coreâ^'shell heterostructure on nickel foam electrode and density functional theory calculations. Journal of Power Sources, 2021, 501, 230003.	7.8	67
63	Synthesis and electrochemical properties of $\hat{l}\pm$ -MnO2 microspheres. Materials Chemistry and Physics, 2008, 109, 399-403.	4.0	66
64	Hollow nitrogen-doped carbon/sulfur@MnO2 nanocomposite with structural and chemical dual-encapsulation for lithium-sulfur battery. Chemical Engineering Journal, 2020, 381, 122746.	12.7	66
65	Uniform Nickel Vanadate (Ni3V2O8) Nanowire Arrays Organized by Ultrathin Nanosheets with Enhanced Lithium Storage Properties. Scientific Reports, 2016, 6, 20826.	3.3	65
66	Probing significant light absorption enhancement of titania inverse opal films for highly exalted photocatalytic degradation of dye pollutants. Applied Catalysis B: Environmental, 2014, 150-151, 411-420.	20.2	64
67	Selenium clusters in Zn-glutamate MOF derived nitrogen-doped hierarchically radial-structured microporous carbon for advanced rechargeable Na–Se batteries. Journal of Materials Chemistry A, 2018, 6, 22790-22797.	10.3	62
68	Facile solution growth of vertically aligned ZnO nanorods sensitized with aqueous CdS and CdSe quantum dots for photovoltaic applications. Nanoscale Research Letters, 2011, 6, 340.	5.7	61
69	Bronze TiO2 as a cathode host for lithium-sulfur batteries. Journal of Energy Chemistry, 2020, 48, 259-266.	12.9	61
70	Porous TiO2 urchins for high performance Li-ion battery electrode: facile synthesis, characterization and structural evolution. Electrochimica Acta, 2016, 210, 206-214.	5.2	60
71	Enhanced Gas Sensitivity and Selectivity on Aperture-Controllable 3D Interconnected Macro–Mesoporous ZnO Nanostructures. ACS Applied Materials & Interfaces, 2016, 8, 8583-8590.	8.0	60
72	Understanding and suppressing side reactions in Li–air batteries. Materials Chemistry Frontiers, 2017, 1, 2495-2510.	5.9	59

#	Article	IF	CITATIONS
73	Self-templated synthesis of microporous CoO nanoparticles with highly enhanced performance for both photocatalysis and lithium-ion batteries. Journal of Materials Chemistry A, 2013, 1, 1394-1400.	10.3	58
74	Core-Shell Structured HMX@Polydopamine Energetic Microspheres: Synergistically Enhanced Mechanical, Thermal, and Safety Performances. Polymers, 2019, 11, 568.	4.5	58
75	Constructing an interface synergistic effect from a SnS/MoS <sub>2</sub> heterojunction decorating N, S co-doped carbon nanosheets with enhanced sodium ion storage performance. Journal of Materials Chemistry A, 2020, 8, 22593-22600.	10.3	58
76	Facile and Rapid Synthesis of Highly Porous Wirelike TiO <sub>2</sub> as Anodes for Lithium-Ion Batteries. ACS Applied Materials & Interfaces, 2012, 4, 1608-1613.	8.0	57
77	Hierarchically structured porous TiO2 spheres constructed by interconnected nanorods as high performance anodes for lithium ion batteries. Chemical Engineering Journal, 2015, 281, 844-851.	12.7	57
78	Engineering 3D bicontinuous hierarchically macro-mesoporous LiFePO4/C nanocomposite for lithium storage with high rate capability and long cycle stability. Scientific Reports, 2016, 6, 25942.	3.3	56
79	Growing NiS2 nanosheets on porous carbon microtubes for hybrid sodium-ion capacitors. Journal of Power Sources, 2020, 451, 227737.	7.8	55
80	MoSe2 nanosheets as a functional host for lithium-sulfur batteries. Journal of Energy Chemistry, 2020, 47, 241-247.	12.9	54
81	Hierarchical Nanotube-Constructed Porous TiO2-B Spheres for High Performance Lithium Ion Batteries. Scientific Reports, 2015, 5, 11557.	3.3	53
82	Unique walnut-shaped porous MnO <sub>2</sub> /C nanospheres with enhanced reaction kinetics for lithium storage with high capacity and superior rate capability. Journal of Materials Chemistry A, 2016, 4, 4264-4272.	10.3	53
83	Coherent TiO <sub>2</sub> /BaTiO <sub>3</sub> heterostructure as a functional reservoir and promoter for polysulfide intermediates. Chemical Communications, 2018, 54, 12250-12253.	4.1	53
84	A MoS <sub>2</sub> @SnS heterostructure for sodium-ion storage with enhanced kinetics. Nanoscale, 2020, 12, 14689-14698.	5.6	53
85	Annealed vanadium oxide nanowires and nanotubes as high performance cathode materials for lithium ion batteries. Journal of Materials Chemistry A, 2014, 2, 14099.	10.3	52
86	Phase-junction Ag/TiO2 nanocomposite as photocathode for H2 generation. Journal of Materials Science and Technology, 2021, 83, 179-187.	10.7	52
87	Hierarchical nanosheet-constructed yolk–shell TiO <sub>2</sub> porous microspheres for lithium batteries with high capacity, superior rate and long cycle capability. Nanoscale, 2015, 7, 12979-12989.	5.6	51
88	Cocatalyzing Pt/PtO Phase-Junction Nanodots on Hierarchically Porous TiO <sub>2</sub> for Highly Enhanced Photocatalytic Hydrogen Production. ACS Applied Materials & Interfaces, 2017, 9, 29687-29698.	8.0	51
89	A flexible, hierarchically porous PANI/MnO <sub>2</sub> network with fast channels and an extraordinary chemical process for stable fast-charging lithium–sulfur batteries. Journal of Materials Chemistry A, 2020, 8, 2741-2751.	10.3	50
90	Facile and fast synthesis of porous TiO2 spheres for use in lithium ion batteries. Journal of Colloid and Interface Science, 2014, 417, 144-151.	9.4	49

#	Article	IF	CITATIONS
91	Enhancing sodium-ion storage performance of MoO2/N-doped carbon through interfacial Mo-N-C bond. Science China Materials, 2021, 64, 85-95.	6.3	48
92	Rutile TiO2 inverse opal with photonic bandgap in the UV–visible range. Journal of Colloid and Interface Science, 2010, 348, 43-48.	9.4	47
93	Facile synthesis of hierarchical and porous V2O5 microspheres as cathode materials for lithium ion batteries. Journal of Colloid and Interface Science, 2014, 418, 74-80.	9.4	47
94	Three-Dimensional (3D) Bicontinuous Hierarchically Porous Mn2O3 Single Crystals for High Performance Lithium-Ion Batteries. Scientific Reports, 2015, 5, 14686.	3.3	47
95	Microwave-assisted hydrothermal synthesis of porous SnO2 nanotubes and their lithium ion storage properties. Journal of Solid State Chemistry, 2012, 190, 104-110.	2.9	46
96	MoSe2 nanoplatelets with enriched active edge sites for superior sodium-ion storage and enhanced alkaline hydrogen evolution activity. Chemical Engineering Journal, 2020, 382, 123047.	12.7	46
97	Unprecedented and highly stable lithium storage capacity of (001) faceted nanosheet-constructed hierarchically porous TiO2/rGO hybrid architecture for high-performance Li-ion batteries. National Science Review, 2020, 7, 1046-1058.	9.5	46
98	Enhanced performance by incorporation of zinc oxide nanowire array for organic-inorganic hybrid solar cells. Applied Physics Letters, 2012, 100, .	3.3	43
99	Smaller Pt particles supported on mesoporous bowl-like carbon for highly efficient and stable methanol oxidation and oxygen reduction reaction. Journal of Power Sources, 2013, 243, 48-53.	7.8	43
100	Probing and suppressing voltage fade of Li-rich Li1.2Ni0.13Co0.13Mn0.54O2 cathode material for lithium-ion battery. Electrochimica Acta, 2019, 318, 875-882.	5.2	42
101	Optimizing inner voids in yolk-shell TiO2 nanostructure for high-performance and ultralong-life lithium-sulfur batteries. Chemical Engineering Journal, 2021, 417, 129241.	12.7	42
102	Chemistry of Trimethyl Aluminum: A Spontaneous Route to Thermally Stable 3D Crystalline Macroporous Alumina Foams with a Hierarchy of Pore Sizes. Chemistry of Materials, 2010, 22, 3251-3258.	6.7	41
103	Understanding Dualâ€Polar Group Functionalized COFs for Accelerating Liâ€Ion Transport and Dendriteâ€Free Deposition in Lithium Metal Anodes. Energy and Environmental Materials, 2023, 6, .	12.8	41
104	Phases Hybriding and Hierarchical Structuring of Mesoporous TiO <sub>2</sub> Nanowire Bundles for Highâ€Rate and Highâ€Capacity Lithium Batteries. Advanced Science, 2015, 2, 1500070.	11.2	39
105	Hierarchical TiO <sub>2</sub> /C nanocomposite monoliths with a robust scaffolding architecture, mesopore–macropore network and TiO <sub>2</sub> –C heterostructure for high-performance lithium ion batteries. Nanoscale, 2016, 8, 10928-10937.	5.6	38
106	Facile synthesis and electrochemical characterization of hierarchical α-MnO2 spheres. Journal of Alloys and Compounds, 2008, 466, 250-257.	5.5	37
107	Stabilizing intermediate phases <i>via</i> the efficient confinement effects of the SnS <sub>2</sub> -SPAN fibre composite for ultra-stable half/full sodium/potassium-ion batteries. Journal of Materials Chemistry A, 2022, 10, 11449-11457.	10.3	36
108	Macroporous ZnO/ZnS/CdS composite spheres as efficient and stable photocatalysts for solar-driven hydrogen generation. Journal of Materials Science, 2017, 52, 11124-11134.	3.7	35

#	Article	IF	CITATIONS
109	Boosting Lithium-Ion Storage Capability in CuO Nanosheets via Synergistic Engineering of Defects and Pores. Frontiers in Chemistry, 2018, 6, 428.	3.6	35
110	A new catalyst for urea oxidation: NiCo2S4 nanowires modified 3D carbon sponge. Journal of Energy Chemistry, 2020, 50, 195-205.	12.9	34
111	Melamine-based polymer networks enabled N, O, S Co-doped defect-rich hierarchically porous carbon nanobelts for stable and long-cycle Li-ion and Li-Se batteries. Journal of Colloid and Interface Science, 2021, 582, 60-69.	9.4	34
112	Facile synthesis of well-shaped spinel LiNi <sub>0.5</sub> Mn <sub>1.5</sub> O <sub>4</sub> nanoparticles as cathode materials for lithium ion batteries. RSC Advances, 2016, 6, 2785-2792.	3.6	32
113	Coherent nanoscale cobalt/cobalt oxide heterostructures embedded in porous carbon for the oxygen reduction reaction. RSC Advances, 2018, 8, 28625-28631.	3.6	32
114	Insight into the positive effect of porous hierarchy in S/C cathodes on the electrochemical performance of Li–S batteries. Nanoscale, 2018, 10, 11861-11868.	5.6	32
115	Topological Insulatorâ€Assisted MoSe <sub>2</sub> /Bi <sub>2</sub> Se <sub>3</sub> Heterostructure: Achieving Fast Reaction Kinetics Toward High Rate Sodiumâ€ion Batteries. ChemElectroChem, 2021, 8, 697-704.	3.4	32
116	Tunable macro–mesoporous ZnO nanostructures for highly sensitive ethanol and acetone gas sensors. RSC Advances, 2015, 5, 101910-101916.	3.6	31
117	Active faceted Cu2O hollow nanospheres for unprecedented adsorption and visible-light degradation of pollutants. Journal of Colloid and Interface Science, 2020, 565, 207-217.	9.4	31
118	Interfacial engineering endowing energetic co-particles with high density and reduced sensitivity. Chemical Engineering Journal, 2020, 387, 124209.	12.7	31
119	Rugated porous Fe3O4 thin films as stable binder-free anode materials for lithium ion batteries. Journal of Materials Chemistry, 2012, 22, 22692.	6.7	30
120	Grain Boundaries Enriched Hierarchically Mesoporous MnO/Carbon Microspheres for Superior Lithium Ion Battery Anode. Electrochimica Acta, 2016, 222, 561-569.	5.2	30
121	Facile synthesis of hierarchically structured manganese oxides as anode for lithium-ion batteries. Journal of Central South University, 2019, 26, 1481-1492.	3.0	29
122	Fine nanoparticles of Al–SnO2 prepared by a co-precipitation route in water/oil microemulsion. Journal of Alloys and Compounds, 2008, 462, 42-46.	5.5	27
123	Seeking a novel energetic co-crystal strategy through the interfacial self-assembly of CL-20 and HMX nanocrystals. CrystEngComm, 2020, 22, 61-67.	2.6	26
124	Synthesis and electrochemical properties of LiMn2O4 and LiCoO2-coated LiMn2O4 cathode materials. Journal of Alloys and Compounds, 2012, 517, 186-191.	5.5	25
125	The mediated synthesis of FeF3 nanocrystals through (NH4)3FeF6 precursors as the cathode material for high power lithium ion batteries. Electrochimica Acta, 2017, 253, 545-553.	5.2	25
126	Nitrogen-doped graphene in-situ modifying MnO nanoparticles for highly improved lithium storage. Applied Surface Science, 2019, 473, 893-901.	6.1	25

#	Article	IF	CITATIONS
127	Dual interface coupled molybdenum diselenide for high-performance sodium ion batteries and capacitors. Journal of Power Sources, 2020, 446, 227298.	7.8	25
128	Interwoven scaffolded porous titanium oxide nanocubes/carbon nanotubes framework for high-performance sodium-ion battery. Journal of Energy Chemistry, 2021, 59, 38-46.	12.9	25
129	Regulating safety and energy release of energetic materials by manipulation of molybdenum disulfide phase. Chemical Engineering Journal, 2021, 411, 128603.	12.7	25
130	Macro/Mesoporous Carbon/Defective TiO <sub>2</sub> Composite as a Functional Host for Lithium–Sulfur Batteries. ACS Applied Energy Materials, 2022, 5, 2573-2579.	5.1	24
131	Three-dimensional ordered hierarchically porous carbon materials for high performance Li-Se battery. Journal of Energy Chemistry, 2022, 68, 624-636.	12.9	23
132	Synchronous Defect and Interface Engineering of NiMoO4 Nanowire Arrays for High-Performance Supercapacitors. Nanomaterials, 2022, 12, 1094.	4.1	23
133	Hollow Cu <sub>2</sub> O microspheres with two active {111} and {110} facets for highly selective adsorption and photodegradation of anionic dye. RSC Advances, 2015, 5, 55520-55526.	3.6	22
134	Multilayer Deposition of Metal–Phenolic Networks for Coating of Energetic Crystals: Modulated Surface Structures and Highly Enhanced Thermal Stability. ACS Applied Energy Materials, 2020, 3, 11091-11098.	5.1	21
135	NiS2 wrapped into graphene with strong Ni-O interaction for advanced sodium and potassium ion batteries. Electrochimica Acta, 2021, 369, 137704.	5.2	21
136	Materials with extreme properties: Their structuring and applications. Vacuum, 2012, 86, 575-585.	3.5	20
137	In Situ Structure Characterization in Slotâ€Dieâ€Printed Allâ€Polymer Solar Cells with Efficiency Over 9%. Solar Rrl, 2019, 3, 1900032.	5.8	20
138	3D interconnected hierarchically macro-mesoporous TiO <sub>2</sub> networks optimized by biomolecular self-assembly for high performance lithium ion batteries. RSC Advances, 2016, 6, 26856-26862.	3.6	19
139	Tin Acceptor Doping Enhanced Thermoelectric Performance of n-Type Yb Single-Filled Skutterudites via Reduced Electronic Thermal Conductivity. ACS Applied Materials & Interfaces, 2019, 11, 25133-25139.	8.0	19
140	Electrochemical fabrication and optical properties of periodically structured porous Fe2O3 films. Electrochemistry Communications, 2012, 20, 178-181.	4.7	18
141	Copper doped CoSx@Co(OH)2 hierarchical mesoporous nanosheet arrays as binder-free electrodes for superior supercapacitors. Journal of Alloys and Compounds, 2022, 911, 165115.	5.5	18
142	Adsorption atalysis onversion of Polysulfides in Sandwiched Ultrathin Ni(OH) <sub>2</sub> â€₽ANI for Stable Lithium–Sulfur Batteries. Small, 2022, 18, .	10.0	18
143	Facile synthesis and electrochemical characterization of Sn4Ni3/C nanocomposites as anode materials for lithium ion batteries. Journal of Solid State Chemistry, 2012, 196, 536-542.	2.9	17
144	Facile synthesis and electrochemical properties of hierarchical MnO2 submicrospheres and LiMn2O4 microspheres. Journal of Physics and Chemistry of Solids, 2007, 68, 1422-1427.	4.0	16

#	Article	IF	CITATIONS
145	Embedding tin disulfide nanoparticles in two-dimensional porous carbon nanosheet interlayers for fast-charging lithium-sulfur batteries. Science China Materials, 2021, 64, 2697-2709.	6.3	16
146	Unprecedented strong and reversible atomic orbital hybridization enables a highly stable Li–S battery. National Science Review, 2022, 9, .	9.5	15
147	Hierarchical porous flower-like TiO 2 -B constructed by thin nanosheets for efficient lithium storage. Materials Letters, 2017, 201, 93-96.	2.6	14
148	Constructing Novel RDX with Hierarchical Structure via Dye-Assisted Solvent Induction and Interfacial Self-Assembly. Crystal Growth and Design, 2020, 20, 4919-4927.	3.0	14
149	Probing the electrochemical behavior of {111} and {110} faceted hollow Cu <sub>2</sub> O microspheres for lithium storage. RSC Advances, 2016, 6, 97129-97136.	3.6	13
150	Fast synthesis of monodisperse TiO2 submicrospheres via a modified sol-gel approach. Rare Metals, 2008, 27, 1-4.	7.1	12
151	Electronic structure at the interfaces of vertically aligned zinc oxide nanowires and sensitizing layers in photochemical solar cells. Journal Physics D: Applied Physics, 2011, 44, 325108.	2.8	12
152	Fresh MoO <sub>2</sub> as a better electrode for pseudocapacitive sodium-ion storage. New Journal of Chemistry, 2018, 42, 14721-14724.	2.8	12
153	Hierarchical Fe <sub>2</sub> O <sub>3</sub> @MoS <sub>2</sub> /C Nanorods as Anode Materials for Sodium Ion Batteries with High Cycle Stability. ACS Applied Energy Materials, 2021, 4, 3757-3765.	5.1	12
154	Tris(trimethylsilyl) borate as electrolyte additive alleviating cathode electrolyte interphase for enhanced lithium-selenium battery. Electrochimica Acta, 2021, 393, 139042.	5.2	12
155	Lithium Storage Performance and Investigation of Electrochemical Mechanism of Cobalt Vanadate Nanowires Assembled by Nanosheets. ACS Applied Energy Materials, 2021, 4, 13401-13409.	5.1	12
156	Facile synthesis of La2Mo2O9 nanoparticles via an EDTA complexing approach. Rare Metals, 2008, 27, 340-344.	7.1	11
157	Alkoxide hydrolysis in-situ constructing robust trimanganese tetraoxide/graphene composite for high-performance lithium storage. Journal of Colloid and Interface Science, 2021, 594, 531-539.	9.4	11
158	NiFe-LDHs@MnO2 heterostructure as a bifunctional electrocatalyst for oxygen-involved reactions and Zn-air batteries. Ionics, 2022, 28, 1273-1283.	2.4	11
159	The chain-mail Co@C electrocatalyst accelerating one-step solid-phase redox for advanced Li–Se batteries. Journal of Materials Chemistry A, 2022, 10, 8059-8067.	10.3	11
160	Exploiting nanostructure-thin film interfaces in advanced sensor device configurations. Vacuum, 2012, 86, 757-760.	3.5	10
161	Amorphous red phosphorus incorporated with pyrolyzed bacterial cellulose as a free-standing anode for high-performance lithium ion batteries. RSC Advances, 2018, 8, 17325-17333.	3.6	10
162	Recent advance on Coâ€based materials for polysulfide catalysis toward promoted lithiumâ€sulfur batteries. Nano Select, 2022, 3, 298-319.	3.7	9

#	Article	IF	CITATIONS
163	High lithium ion battery performance enhancement by controlled carbon coating of TiO <sub>2</sub> hierarchically porous hollow spheres. RSC Advances, 2016, 6, 70485-70492.	3.6	8
164	TiO2/Sb2S3/P3HT Based Inorganic–Organic Hybrid Heterojunction Solar Cells with Enhanced Photoelectric Conversion Performance. Journal of Electronic Materials, 2017, 46, 4670-4675.	2.2	8
165	Sodium-ion storage mechanisms and design strategies of molybdenum-based materials: A review. Applied Materials Today, 2021, 23, 100985.	4.3	8
166	Enhanced Short-Wavelength Absorption and Effective Exciton Dissociation in NC70BA-Based Ternary Polymer Solar Cells. ACS Applied Energy Materials, 2021, 4, 8432-8441.	5.1	7
167	Phase Conversion Accelerating "Znâ€Escape―Effect in ZnSeâ€CFs Heterostructure for High Performance Sodiumâ€Ion Half/Full Batteries. Small, 2022, 18, 2105169.	10.0	7
168	Two Better Compatible and Complementary Light Absorption Polymer Donors Contributing Synergistically to High Efficiency and Better Thermally Stable Ternary Organic Solar Cells. ACS Applied Energy Materials, 0, , .	5.1	7
169	Dual catalysis-adsorption function modified separator towards high-performance Li-Se battery. Applied Surface Science, 2022, 599, 153932.	6.1	7
170	Ternary polymer solar cells by employing two well-compatible donors with cascade energy levels. Dyes and Pigments, 2021, 192, 109424.	3.7	5
171	Gradient selenium-doping regulating interfacial charge transfer in zinc sulfide/carbon anode for stable lithium storage. Journal of Colloid and Interface Science, 2022, 619, 42-50.	9.4	5
172	Pt-Modified Interfacial Engineering for Enhanced Photocatalytic Performance of 3D Ordered Macroporous TiO2. Crystals, 2022, 12, 778.	2.2	5
173	Understanding the effect of the double side chain fullerene derivative as third component materials on the charge dynamics and photovoltaic performance. Solar Energy, 2021, 230, 549-557.	6.1	4
174	Ternary organic solar cells with double side chain fullerene derivative as guest electron acceptors in PM7:Y6 blend films. Organic Electronics, 2022, 103, 106465.	2.6	4
175	Porous MoS <sub>2</sub> nanosheets for the fast decomposition of energetic compounds. Dalton Transactions, 2022, 51, 5278-5284.	3.3	4
176	Inverted Nonfullerene Polymer Solar Cells with Photoannealed Cs <sub>2</sub> CO <sub>3</sub> Films as Electron Extraction Layers. Advanced Electronic Materials, 2022, 8, .	5.1	4
177	Boosting reaction kinetics and shuttle effect suppression by single crystal MOF-derived N-doped ordered hierarchically porous carbon for high performance Li-Se battery. Science China Materials, 2022, 65, 2975-2988.	6.3	4
178	Improving all ternary small-molecule organic solar cells by optimizing short wavelength photon harvesting and exciton dissociation based on a bisadduct analogue of [70]PCBM as a third component material. Sustainable Energy and Fuels, 2022, 6, 744-755.	4.9	3
179	Two Well-Compatible Acceptors with Red-Shifted Absorption Edge and Cascaded LUMO Levels Enable Ternary Organic Photovoltaic Exhibiting Efficient Photovoltaic Performance. ACS Applied Energy Materials, 2022, 5, 1076-1084.	5.1	2
180	SnO2 nano-mulberries anchored onto RGO nanosheets for lithium ion batteries. Journal of Materials Research, 2020, 35, 20-30.	2.6	1

#	Article	IF	CITATIONS
181	High-performance ternary organic photovoltaics with NC <sub>70</sub> BA as the third component material enabling thickness-insensitive photoactive performance. Nanotechnology, 2022, 33, 065206.	2.6	1
182	Ternary organic photovoltaics with good thickness tolerance by NC70BA as the third component. Organic Electronics, 2022, 100, 106397.	2.6	1
183	High efficiency inverted organic solar cells with photo annealing titanium oxide films as electron extract layer. Colloids and Surfaces A: Physicochemical and Engineering Aspects, 2022, 642, 128698.	4.7	1
184	Fabrication of Zn-Cu-Ni Ternary Oxides in Nanoarrays for Photo-Enhanced Pseudocapacitive Charge Storage. Nanomaterials, 2022, 12, 2457.	4.1	1